

# Characteristics of Longitudinal and Torsional Vibration for Hole Machining by Ultrasonic Vibration

Takuya Asami (1), Hikaru Miura (1)

(1) Department of Electrical Engineering, College of Science and Technology, Nihon University;

1-8-14, Kanda Surugadai, Chiyoda-ku, Tokyo, 101-8308, Japan; taku.asami@gmail.com

PACS: 43.35.Zc

## ABSTRACT

We are developing a new method using ultrasonic longitudinal and torsional vibration of a hollow-type stepped horn for hole machining. We foresee that the equipment can be simplified and miniaturized. In this paper, ultrasonic vibration sources of a hollow-type stepped horn without a diagonal slits vibration converter and with a diagonal slits vibration converter are used. The longitudinal and torsional vibration characteristics of the horn are clarified and the shape of the horn is examined. First, the longitudinal vibration characteristics of a hollow-type stepped horn without diagonal slits are clarified. As a result, the hollow-typed stepped horn has the best shape in all cases of the cross-sectional ratio when the hollow part depth is  $1/4$  wavelength. The amplification factor was decided by the cross-sectional ratio when the hollow part depth is  $1/4$  wavelength. The amplification factors are proportional to the cross-sectional ratio, but if the amplification factor exceeds 4.6, it was not proportional to the cross-sectional ratio. The longitudinal vibration adding the static pressing force has a resonance of  $1/2$  wavelength for this hollow-type stepped horn length in all cases. Second, the longitudinal and torsional vibration characteristics of a hollow-type stepped horn with diagonal slits are clarified. As a result, the longitudinal vibration amplitude is proportional to the cross-sectional ratio, but the torsional vibration amplitude is the same value in all cases of cross-sectional ratio. The torsional vibration amplitude of the tip side becomes larger when the hollow part contains diagonal slits.

## 1. INTRODUCTION

Ceramic materials are used for many purposes, but the material processing methods still face some problems. Currently, laser, water jet and wire electric discharge machining are used for hole machining of brittle material such as ceramics materials. The advantages of these methods are higher removal rate and machining accuracy. However, the disadvantages are that conventional equipment is large and the structure is complex.

To resolve this issue, a new method using the ultrasonic longitudinal and torsional vibration of a hollow-type stepped horn for hole machining is developed [1], [2]. We foresee that with this method equipment can be simplified and miniaturized. In this paper, ultrasonic vibration sources of a hollow-type stepped horn without a diagonal slits vibration converter and with a diagonal slits vibration converter are used. The longitudinal and torsional vibration characteristics of the horn are clarified and the shape of the horn is examined.

First, the characteristics of longitudinal vibration of the hollow-type stepped horn without diagonal slits are discussed. The shape of the horn without diagonal slits was examined via experiments on the longitudinal vibration distribution of the horn and the longitudinal vibration amplification factor. The characteristics of the longitudinal vibration of the horn were examined when the static pressing force at the tip of the horn is varied.

Second, the characteristics of longitudinal and torsional vibration of the hollow-type stepped horn with diagonal slits are discussed. The shape of the hollow-type stepped horn with diagonal slits was examined.

## 2. ULTRASONIC VIBRATION SOURCE

Figure 1 shows the ultrasonic vibration source. The ultrasonic vibration source consists of a 20 kHz bolt-clamped Langevin-type transducer, an exponential horn for amplitude amplification (length, 155 mm; large-end diameter, 55 mm; small-end diameter, 12 mm; amplification factor, approximately 4.7; material, duralumin), and a hollow-type stepped horn, with dimensions as shown in Fig. 2.

Figure 2(a) shows the longitudinal vibration of the hollow-type stepped horn without a diagonal slits vibration converter. Fig. 2(b) shows the longitudinal and torsional vibration of the hollow-type stepped horn with a diagonal slits vibration converter. The dimensions of the hollow-type stepped horn in Fig. 2(a) are as follows: length,  $(L_1+L_2)$  120 mm ( $\lambda/2$  is constant, where  $\lambda$  is defined as the longitudinal vibration wavelength at 20 kHz); cross-sectional area of transducer side  $S_1$ , 113 mm<sup>2</sup> (diameter 12 mm); cross-sectional area of tip side,  $S_2$ ; depth of the hollow part,  $L_2$ ; cross-sectional ratio, transducer-side cross-sectional area  $S_1$ / tip-side cross-sectional area  $S_2$ .

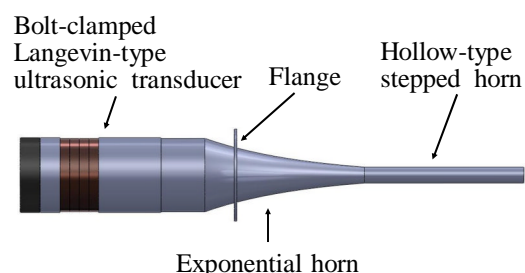


Figure 1. Ultrasonic vibration source

The dimensions of the other horn shown in Fig. 2(b) are the same as those of the horn without diagonal slits. The exterior appearance of the diagonal slits is shown in Fig. 3.

### 3. MEASUREMENT METHODS OF LONGITUDINAL AND TORSIONAL VIBRATION DISTRIBUTION

The longitudinal vibration of the hollow-type stepped horn at the measurement position  $x$  was measured using a ring-type magnetic ultrasonic vibration detector, as shown in Fig. 4, with the following dimensions: thickness, 11 mm; outside diameter, 40 mm; inside diameter, 13 mm. The detector output voltage is induced by eddy currents produced by magnetic flux and the vibration of the vibrating surface, and is proportional to the vibration velocity amplitude [3]. Two coils are connected in series with antiphase polarity. The detector output voltage was verified using a laser Doppler vibrometer (Ono Sokki, LV-1710).

Also, the torsional vibration of the hollow-type stepped horn at the measurement position  $x$  was measured using the same laser Doppler vibrometer.

## 4. CHARACTERISTICS OF LONGITUDINAL VIBRATION OF THE HOLLOW-TYPE STEPPED HORN WITHOUT DIAGONAL SLIT PARTS

### 4.1 Longitudinal vibration distribution

To obtain excellent hole machining properties, the shape of the hollow-type stepped horn should be examined [4]. To study the longitudinal vibration distribution, the longitudinal vibration at measurement position  $x$  was measured by varying the depth of the hollow part  $L_2$  ( $L_1=120-L_2$ ) in the range of 50-70 mm at 5 mm intervals and making cross-sectional ratios of 2, 3, and 4 (the cross-sectional area of the hollow part  $S_2$  equal to 56.4, 37.7, and 28.1 mm<sup>2</sup>, respectively. These values remain the same for other experiments discussed in this paper). The experiment was conducted with the longitudinal vibration amplitude of the transducer side fixed at 0.2 μm (effective value).

Figures 5(a)-5(c) show the longitudinal vibration distribution for cross-sectional ratios of 2, 3, and 4, respectively. The vertical and horizontal axes in Fig. 5 represent the longitudinal vibration amplitude (0 to peak value) and the measurement position  $x$ , respectively. According to Fig. 5, the loop

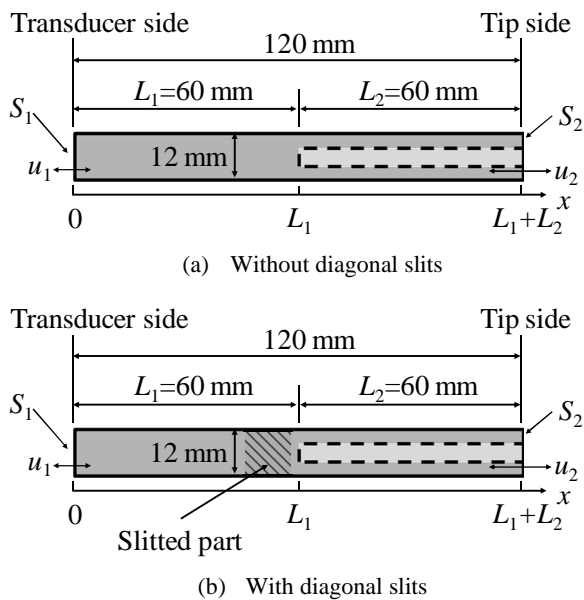


Figure 2. Hollow-type stepped horn

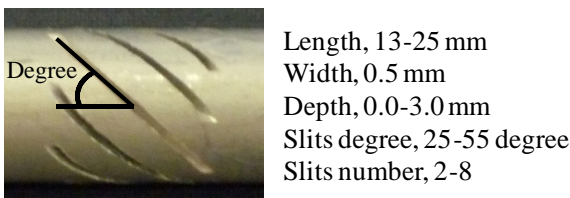


Figure 3. Appearance of the diagonal slit part

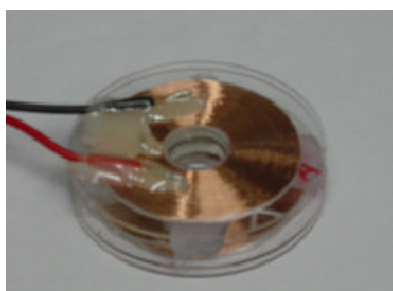


Figure 4. Ring-type magnetic ultrasonic vibration detector

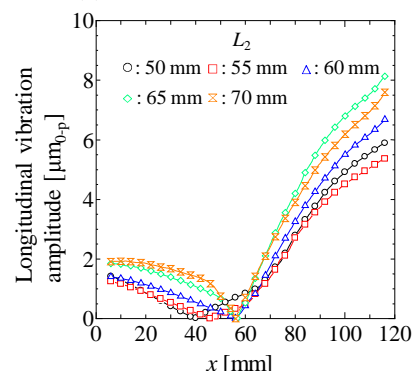
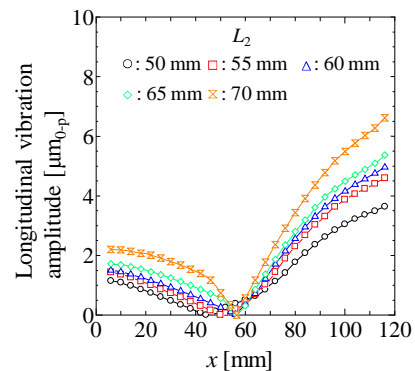
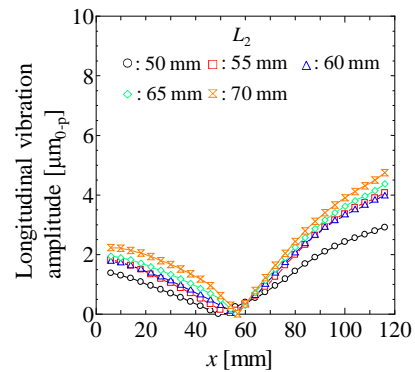


Figure 5. Longitudinal vibration distribution

positions of the longitudinal vibration amplitude are at the transducer side ( $x=0$  mm) and at the tip ( $x=120$  mm), and the node position is at  $x=49-56$  mm. The longitudinal vibration has a resonance frequency corresponding to half of the wavelength for this length of hollow-type stepped horn. This result indicates that the longitudinal vibration distribution is affected by the length of the hollow part  $L_2$ . We assume that this was because the stress distribution varied with  $L_2$ . The larger the cross-sectional area of the cross-sectional ratio, the larger the longitudinal vibration amplitude at the tip ( $x=120$  mm) becomes.

Figure 6 shows the relationship between the node position of the longitudinal vibration distribution in Fig. 4 and the depth of the hollow part  $L_2$ . According to Fig. 5, the node position changes markedly when  $L_2$  increases from 50 to 55 mm for all values of cross-sectional ratio. In contrast, the node position was similar for  $L_2=60, 65,$  and  $70$  mm for all values of  $S_2$ .

Figure 7 shows the relationship between the resonance frequency and  $L_2$ . The vertical and horizontal axes in Fig. 6 represent the resonance frequency and  $L_2$ , respectively. According to Fig. 6, the resonance frequency decreases with increasing  $L_2$ . When  $L_2$  was 50, 55, 65, and 70 mm the resonance frequency varied with the cross-sectional ratio. In contrast, the resonance frequency was almost the same value for different values of cross-sectional ratio when  $L_2$  was 60 mm.

#### 4.2 Relationship between the depth of hollow part $L_2$ and the longitudinal vibration amplification factor

To obtain a high longitudinal vibration amplitude at the tip of a hollow-type stepped horn, the shape of the horn should be examined. To study the relationship between  $L_2$  and the amplification factor, the longitudinal vibration at the tip of the horn was measured by varying  $L_2$  in the range of 50-70 mm at 2 mm intervals and making the cross-sectional ratios of 2, 3, and 4. A transducer was fixed at 100 mA.

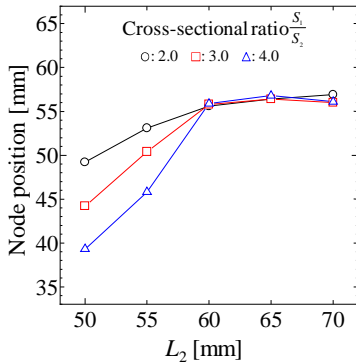


Figure 6. Relationship between  $L_2$  and node position

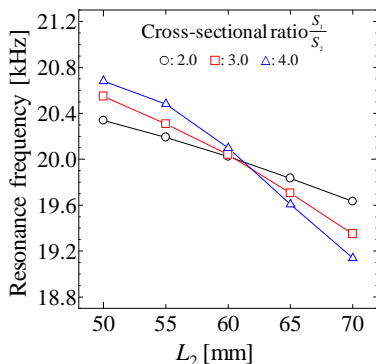


Figure 7. Relationship between  $L_2$  and resonance frequency

Figure 8 shows the results. The vertical and horizontal axes in Fig. 8 represent the longitudinal vibration amplification factor (longitudinal vibration at the tip / longitudinal vibration at the transducer side) and the depth of the hollow part  $L_2$ , respectively. According to Fig. 4, the amplification factor reaches a maximum when  $L_2=60$  mm, independent of cross-sectional ratio.

#### 4.3 Relationship between cross-sectional ratio and the longitudinal vibration amplification factor

To study the relationship between the cross-sectional ratio of the hollow-type stepped horn and the longitudinal vibration amplification factor, the longitudinal vibration at the tip of the horn was measured by varying the cross-sectional area of the hollow part  $S_2$ , as shown in Table I. The experiment was conducted with the longitudinal vibration amplitude of the transducer side fixed at  $1.0 \mu\text{m}$  (effective value) and  $L_2$  fixed

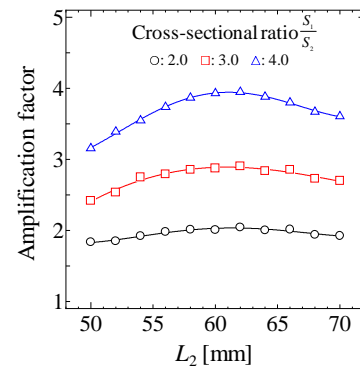


Figure 8. Relationship between  $L_2$  and amplification factor

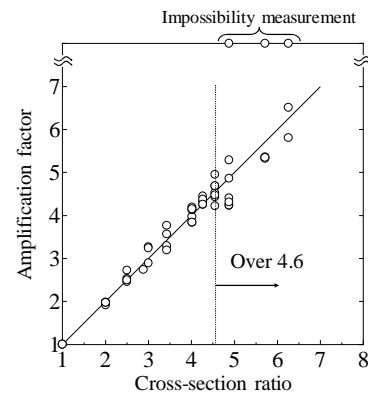


Figure 9. Relationship between cross-sectional ratio and amplification factor

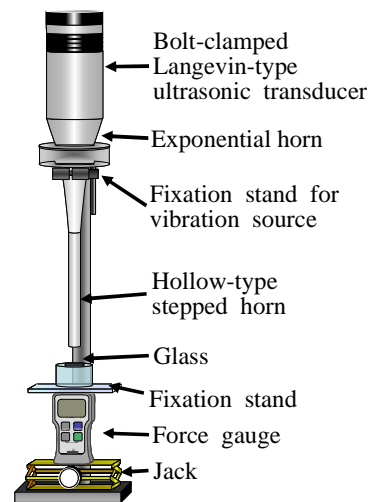
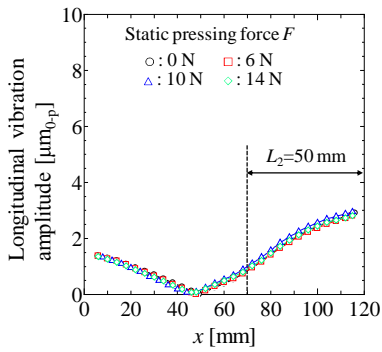
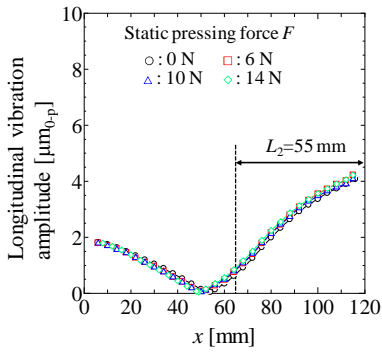


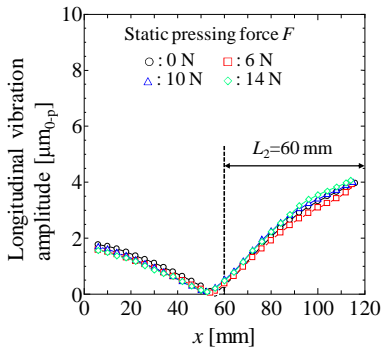
Figure 10. Experimental apparatus



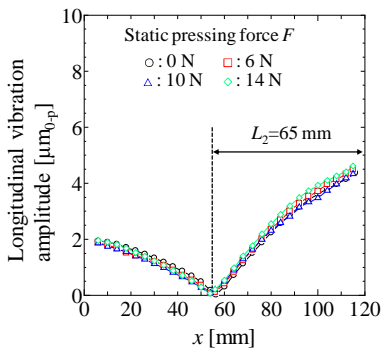
(a)  $L_2=50$  mm



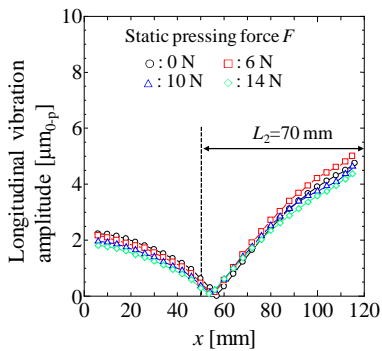
(b)  $L_2=55$  mm



(c)  $L_2=60$  mm

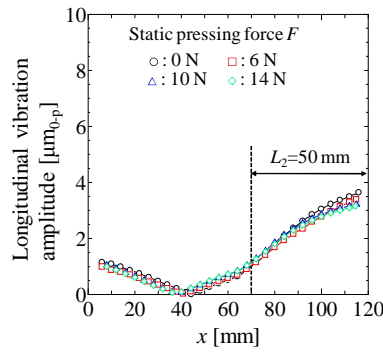


(d)  $L_2=65$  mm

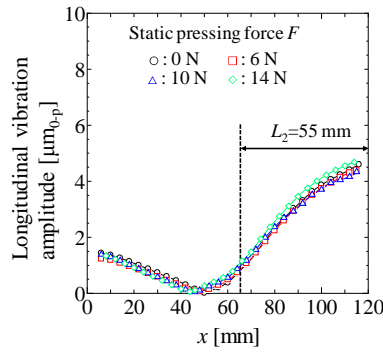


(e)  $L_2=70$  mm

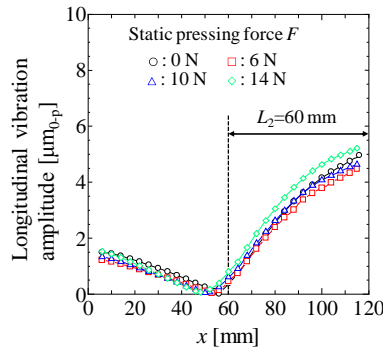
**Figure 11.** Longitudinal vibration distribution (Cross-sectional ratio 2)



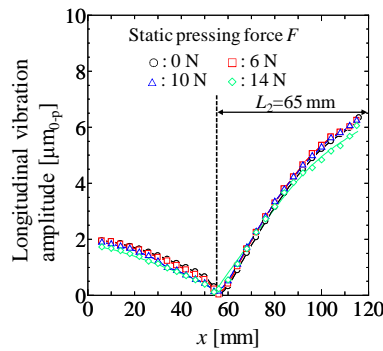
(a)  $L_2=50$  mm



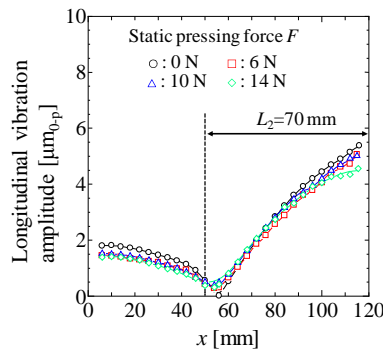
(b)  $L_2=55$  mm



(c)  $L_2=60$  mm

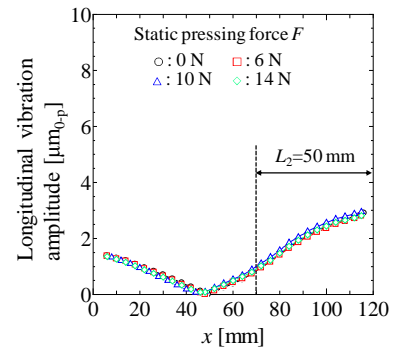


(d)  $L_2=65$  mm

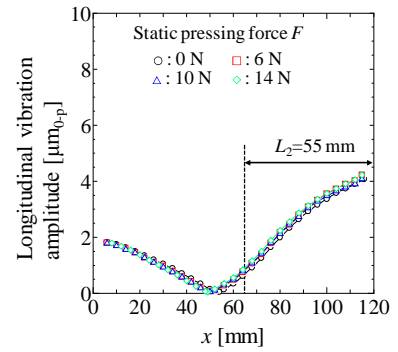


(e)  $L_2=70$  mm

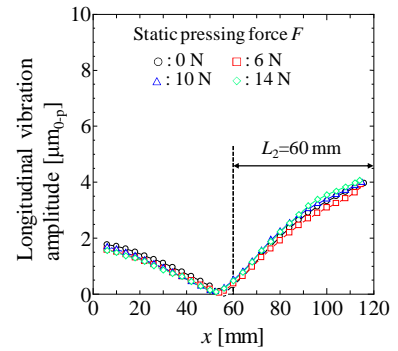
**Figure 12.** Longitudinal vibration distribution (Cross-sectional ratio 3)



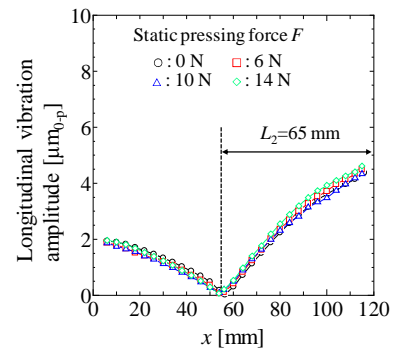
(a)  $L_2=50$  mm



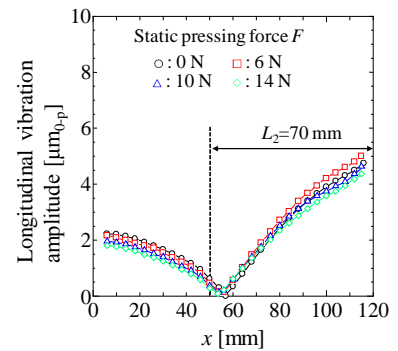
(b)  $L_2=55$  mm



(c)  $L_2=60$  mm



(d)  $L_2=65$  mm



(e)  $L_2=70$  mm

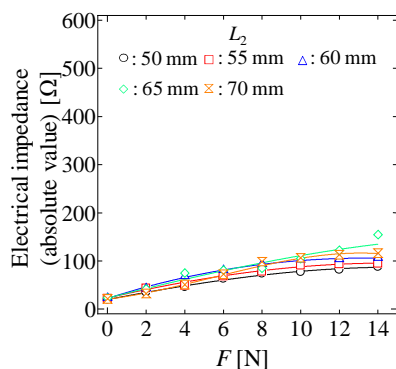
**Figure 13.** Longitudinal vibration distribution (Cross-sectional ratio 4)

at 60 mm.

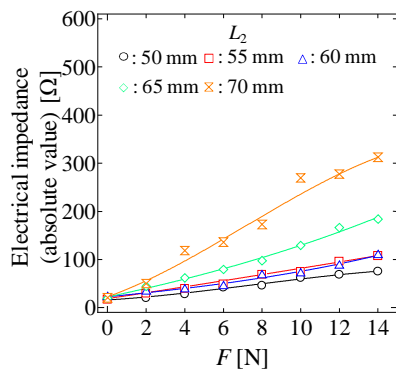
**Table I.** Relationship between cross-sectional area  $S_2$  and cross-sectional ratio

$S_2$ (mm <sup>2</sup> )	113.1	56.4	45.2	37.7	33.0	28.1	26.5	24.9	23.2	19.8	18.1
Cross-sectional ratio	1.0	2.0	2.5	3.0	3.4	4.0	4.3	4.6	4.9	5.7	6.3

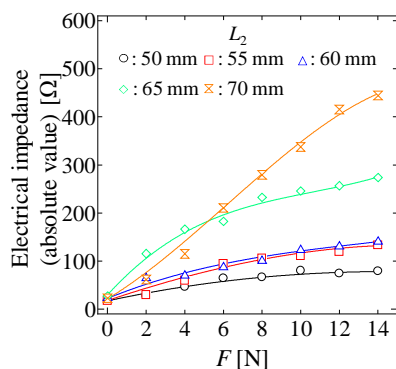
Figure 9 shows the results. The vertical and horizontal axes in Fig. 9 respectively represent the longitudinal vibration amplification factor (longitudinal vibration amplitude at the tip / longitudinal vibration amplitude at the tip of a uniform rod) and the cross-sectional ratio. According to Fig. 9, the longitudinal vibration amplification factor is proportional to the cross-sectional ratio provided the longitudinal vibration cross-sectional ratio does not exceed 4.6. Some ultrasonic vibration sources of the horn do not resonate provided the cross-sectional ratio exceeds 4.6, i.e., some longitudinal vibration amplification factors are impossible to measure. This result indicates that the longitudinal vibration is not transmitted at the boundary of the solid part and the hollow part when  $L_2=60$  mm and the cross-sectional ratio exceeds 4.6.



(a) Cross-sectional ratio 2



(b) Cross-sectional ratio 3



(c) Cross-sectional ratio 4

**Figure 14.** Relationship between static pressing force  $F$  and impedance

#### 4.4 Characteristics of longitudinal vibration when static pressing force $F$ is varied

We compared the characteristics of the longitudinal vibration of the hollow-type stepped horn for different values of  $F$  with those when no force is applied. The longitudinal vibration at the measurement position  $x$  and the electrical impedance (absolute value) of the ultrasonic vibration source were measured by varying  $L_2$  in the range of 50-70 mm at 5 mm intervals, making the cross-sectional ratios of 2, 3, and 4, and varying  $F$  in the range of 0-14 N. The experiment was conducted with the longitudinal vibration amplitude of the transducer side fixed at 0.2  $\mu\text{m}$ . Also, the electrical impedance (absolute value) of the ultrasonic vibration source was obtained from the supply current, the supply voltage of the transducer, and the phase. Figure 10 shows the apparatus used to examine the effect of applying static pressing force  $F$  at the tip of the hollow-type stepped horn. A constant force is applied to the tip of the horn from the lower side of the fixation stand to maintain contact between the glass and the tip of the horn.

Figures 11-13 show the longitudinal vibration distributions for cross-sectional ratios of 2, 3, and 4. In each figure, (a)-(e) show the results for  $L_2=50, 55, 60, 65,$  and  $70$  mm, respectively. The vertical and horizontal axes in Figs. 11-13 represent the longitudinal vibration amplitude (effective value) and the measurement position  $x$ , respectively. According to these figures, the loop positions of the longitudinal vibration amplitude are at the transducer side ( $x=0$  mm) and at the tip ( $x=120$  mm), and the node position is near  $x=60$  mm. The longitudinal vibration has a resonance frequency corresponding to half of the wavelength for this length of hollow-type stepped horn in all cases. Also, the distribution when the static pressing force  $F$  was applied was similar to that when no static pressing force was applied. The longitudinal vibration distribution, node position, and resonance frequency were hardly affected by the magnitude of  $F$ . We assume that this was because the tip side was nearly free and not fixed.

Figure 14 shows the relationship between  $F$  and electrical impedance (absolute value). Figures 14(a)-14(c) show the results for cross-sectional ratios of 2, 3, and 4. The vertical and horizontal axes in Fig. 13 represent the impedance and  $F$ , respectively. According to Fig. 14, impedance increased with  $F$  for all values of cross-sectional ratio. Also, impedance increased with cross-sectional ratio.

### 5. CHARACTERISTICS OF LONGITUDINAL AND TORSIONAL VIBRATION OF THE HOLLOW-TYPE STEPPED HORN WITH DIAGONAL SLIT PARTS

#### 5.1 The longitudinal and torsional vibration distribution of the uniform rod with diagonal slit parts

To study the longitudinal and torsional vibration distribution of the uniform rod (length, 120 mm; diameter, 12 mm), the longitudinal and torsional vibration distribution of the horn was measured. The experiment was conducted with the longitudinal vibration amplitude of the transducer side fixed at 0.2  $\mu\text{m}$  (effective value). Slit conditions are as follows: length, 15 mm; width, 0.5 mm; depth, 0.0-3.0 mm; degree, 45 deg; number, 8; center position  $x$  of the slit part, 58 mm. The experiment was done as a pre-experiment.

Figure 15 shows the longitudinal and torsional vibration distribution. The vertical and horizontal axes in Fig. 15 represent the longitudinal and torsional vibration amplitude (0 to peak value) and the measurement position  $x$ , respectively.

According to Fig. 15, the longitudinal vibration has a resonance frequency corresponding to half of the wavelength for this rod. The loop positions of the torsional vibration amplitude are at  $x=32$  mm and at the tip ( $x=120$  mm), and the node position is at the transducer side ( $x=0$  mm) and at  $x=80$  mm. The torsional vibration has a resonance frequency corresponding to three-quarter of the wavelength for this length of rod.

### 5.2 Relationship between cross-sectional ratio and the longitudinal and torsional vibration distribution

To study the relationship between the cross-sectional ratio of the hollow-type stepped horn and the longitudinal and torsional vibration distribution, the longitudinal and torsional vibration distribution of the horn was measured by making the cross-sectional ratios of 1, 2, 3, and 4 (the cross-sectional area of the hollow part  $S_2$  equal to 113.1, 56.4, 37.7, and 28.1  $\text{mm}^2$ , respectively). A horn with cross-sectional ratio equal to 1 is uniform rod for reference. The experiment was conducted with the longitudinal vibration amplitude of the transducer side fixed at  $0.2 \mu\text{m}$  (effective value),  $L_2$  fixed at 60 mm. Slit conditions are as follows: length, 15 mm; width, 0.5

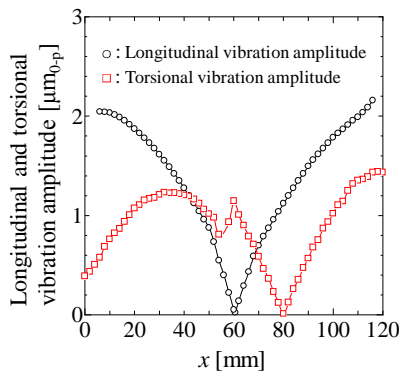


Figure 15. Longitudinal and torsional vibration distribution of uniform rod

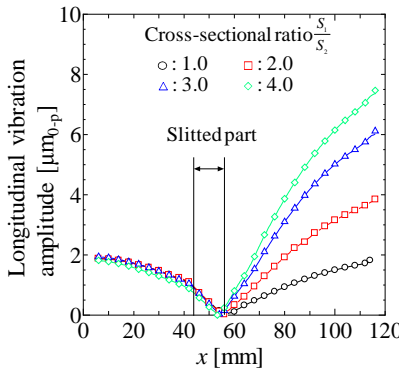


Figure 16. Longitudinal vibration distribution when varying the cross-sectional

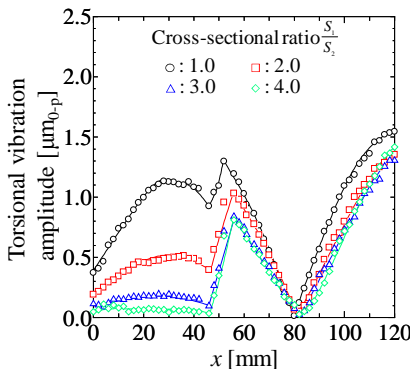


Figure 17. Torsional vibration distribution when varying the cross-sectional ratio

mm; depth, 0.0~3.0 mm; degree, 45 deg; number, 8; center position  $x$  of the slit part, 50 mm.

Figure 16 shows the longitudinal vibration distribution. The vertical and horizontal axes in Fig. 16 represent the longitudinal vibration amplitude (0 to peak value) and the measurement position  $x$ , respectively. According to Fig. 16, the longitudinal vibration has a resonance frequency corresponding to half of the wavelength for this length of hollow-type stepped horn. This result indicates that the longitudinal vibration distribution is affected by the cross-sectional ratio. The larger the cross-sectional ratio, the larger the longitudinal vibration amplitude at the tip ( $x=120$  mm) becomes. We assume that this was due to the variation of the longitudinal vibration amplification factor with cross-sectional ratio.

Figure 17 shows the torsional vibration distribution. The vertical and horizontal axes in Fig. 17 represent the torsional vibration amplitude (0 to peak value) and the measurement position  $x$ , respectively. According to Fig. 17, the torsional vibration has a resonance frequency corresponding to three-quarter of the wavelength for this length of hollow-type stepped horn. The larger the cross-sectional ratio, the smaller the range of  $x=0-44$  mm of the torsional vibration distribution becomes. In the range of  $x=56-120$  mm, the torsional vibration distribution was the same distribution for different values of cross-sectional ratio. The torsional vibration at the tip side was the same value for different values of cross-sectional ratio. This result indicates that the torsional vibration amplification factor was not affected by different values of cross-sectional ratio.

### 5.3 Relationship between degree of slits and the longitudinal and torsional vibration distribution

To obtain a high torsional vibration amplitude at the tip of the horn, the longitudinal and torsional vibration distributions of the horn was measured by varying the degree of slits in the range of 25-55 degrees (length of slits in the range of 25-13 mm) at 10 degree intervals. The experiment was conducted

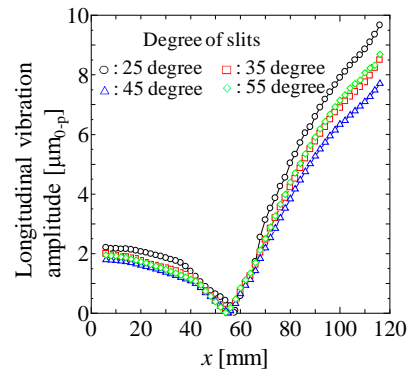


Figure 18. Longitudinal vibration distribution when varying the degree of slits

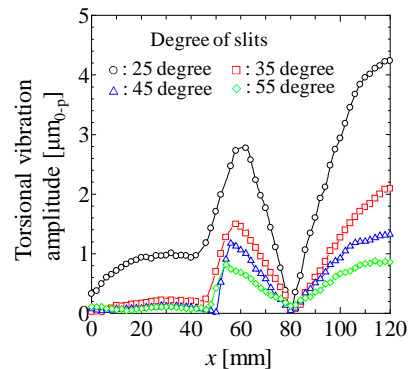


Figure 19. Torsional vibration distribution when varying the degree of slits

with the longitudinal vibration amplitude of the transducer side fixed at  $0.2 \mu\text{m}$  (effective value),  $L_2$  fixed at 60 mm, the cross-sectional ratios of 4 ( $S_2$  fixed  $28.1 \text{ mm}^2$ ). Slit conditions are as follows: width, 0.5 mm; depth, 0.0~3.0 mm; number, 8; center position  $x$  of the slit part, 50 mm.

Figure 18 shows the longitudinal vibration distribution. The vertical and horizontal axes in Fig. 18 represent the longitudinal vibration amplitude (0 to peak value) and the measurement position  $x$ , respectively. According to Fig. 18, the longitudinal vibration amplitude of the tip side reached maximum value when the degree of the slits was equal to 25 degrees. The longitudinal vibration amplification factor was larger than the cross-sectional ratio when the degree of the slits was equal to 25 degrees. We assume that this was due to that the 25 degree slits bore the hollow part. The longitudinal vibration distributions of degree of slits in the range of 35-55 degrees were hardly affected by the degree of the slits.

Figure 19 shows the torsional vibration distribution. The vertical and horizontal axes in Fig. 19 represent the torsional vibration amplitude (0 to peak value) and the measurement position  $x$ , respectively. According to Fig. 19, the torsional vibration has a resonance frequency corresponding to three-quarter of the wavelength for this length of hollow-type stepped horn in all cases of slits degree. The smaller the slits degree, the larger the torsional vibration amplitude value of the tip side becomes. We assume that this was due to that the ratio from which longitudinal vibration was converted into torsional vibration increased when slit part approaches the hollow part of the horn and the node position of the longitudinal vibration. The torsional vibration amplitude of the tip side reached maximum value when the slits degree was equal to 25 degrees. We assume that this was due to that the slits bore the hollow part when the degree of slits was equal to 25 degrees.

#### 5.4 Relationship between number of diagonal slits and the longitudinal and torsional vibration distribution

To study the relationship between the number of slits and the longitudinal and torsional vibration distribution, the longitudinal and torsional vibration distribution of the horn was measured by varying the number of slits in the range of 2-8 at 2 intervals. The experiment was conducted with the longitudinal vibration amplitude of the transducer side fixed at  $0.2 \mu\text{m}$  (effective value),  $L_2$  fixed at 60 mm, the cross-sectional ratios of 4 ( $S_2$  fixed  $28.1 \text{ mm}^2$ ). Slit conditions are as follows: length, 15 mm; width, 0.5 mm; depth, 0.0~3.0 mm; degree, 45 deg; center of slit part  $x$ , 50 mm.

Figure 20 shows the longitudinal vibration distribution. The vertical and horizontal axes in Fig. 20 represent the longitudinal vibration amplitude (0 to peak value) and the measurement position  $x$ , respectively. According to Fig. 20, the longitudinal vibration has a resonance frequency corresponding to half of the wavelength for this length of hollow-type stepped horn. This result indicates that the longitudinal vibration distribution is hardly affected by the number of slits.

Figure 21 shows the torsional vibration distribution. The vertical and horizontal axes in Fig. 21 represent the torsional vibration amplitude (0 to peak value) and the measurement position  $x$ , respectively. According to Fig. 21, the torsional vibration has a resonance frequency corresponding to three-quarter of the wavelength for this length of hollow-type stepped horn unrelated to the number of slits. The torsional vibration amplitude of the tip side increased with the number of slits. The torsional vibration distribution in the range of  $x=0-40 \text{ mm}$  attenuated unrelated to the number of slits. For this reason, the cross-sectional ratio was equal to 4.

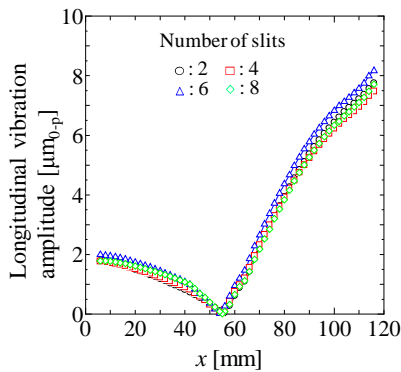


Figure 20. Longitudinal vibration distribution when varying the number of slits

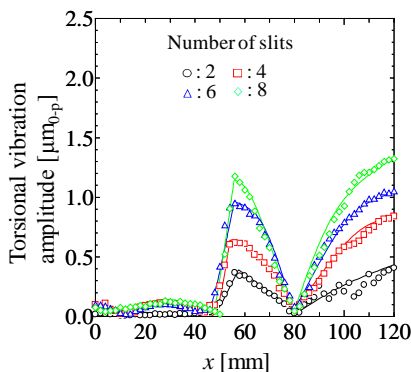


Figure 21. Torsional vibration distribution when varying the number of slits

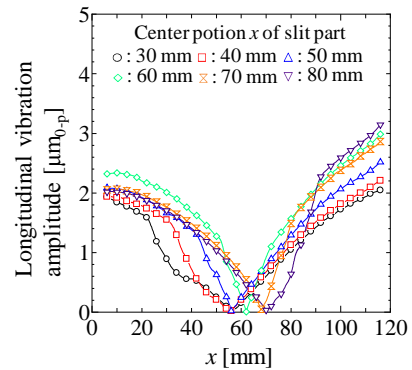


Figure 22. Longitudinal vibration distribution when varying the center position  $x$  of slit part

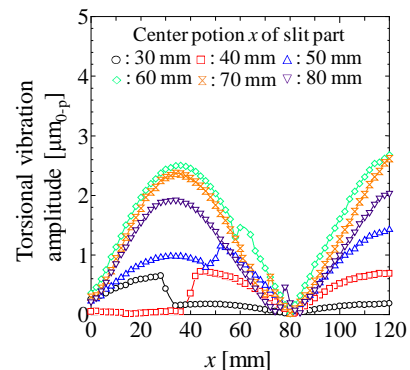


Figure 23. Torsional vibration distribution when varying the center position  $x$  of slit part

### 5.5 Relationship between center of slit part $x$ and the longitudinal and torsional vibration distribution

To study the relationship between the center position  $x$  of the slit part and the longitudinal and torsional vibration distributions, the longitudinal and torsional vibration distributions of the horn was measured by varying the center position  $x$  of the slit part in the range of 30-80 mm at 10 intervals. The experiment was conducted with the longitudinal vibration amplitude of the transducer side fixed at  $0.2 \mu\text{m}$  (effective value),  $L_2$  fixed at 60 mm, cross-sectional ratio of 1.2 ( $S_2$  fixed  $93.5 \text{ mm}^2$ ). Slit conditions are as follows: length, 15 mm; width, 0.5 mm; depth, 0.0~3.0 mm; degree, 45 deg; number, 8.

Figure 22 shows the longitudinal vibration distribution. The vertical and horizontal axes in Fig. 22 represent the longitudinal vibration amplitude (0 to peak value) and the measurement position  $x$ , respectively. According to Fig. 22, the longitudinal vibration distribution and the node position of longitudinal vibration were affected by the center position  $x$  of the slit part. The longitudinal vibration amplitude value of the tip side increased when the center position  $x$  of slit part approaches the tip of the horn. The node position of the longitudinal vibration was hardly affected when the center position  $x$  was equal to 30-50 mm. By contrast, the node position of longitudinal vibration was affected when the center position  $x$  was equal to 60-80 mm. This result indicates that the influence on longitudinal vibration distribution by the center position of the slit part is large when the hollow part contains diagonal slits.

Figure 23 shows the torsional vibration distribution. The vertical and horizontal axes in Fig. 23 represent the torsional vibration amplitude (0 to peak value) and the measurement position  $x$ , respectively. According to Fig. 23, the torsional vibration distribution was affected in the all cases of center position  $x$  of slit part. Nevertheless, the torsional vibration has a resonance frequency corresponding to three-quarter of the wavelength for this length of hollow-type stepped horn. The torsional vibration amplitude of the tip side reached the maximum value when center position  $x$  of slit part was equal to 60 mm. We assume that this was due to that the slit part contained the hollow part and was near the node position of longitudinal vibration. The torsional vibration distribution in the range of  $x=0-40$  mm attenuated when center position  $x$  of slit part was equal to 40 mm.

## 6. CONCLUSIONS

The shape of a hollow-type stepped horn and the characteristics of longitudinal and torsional vibration required to obtain excellent hole machining properties were investigated in

cases of a horn with and without diagonal slits. First, in the case of a horn without diagonal slits, we found that the resonance frequency of the hollow-type stepped horn had the same value regardless of the cross-sectional ratio when the depth of the hollow part was  $L_2=60$  mm. The amplification factor was only determined by the cross-sectional ratio when  $L_2$  was 60 mm. The hollow-type stepped horn with  $L_2=60$  mm has excellent longitudinal vibration for all values of the cross-sectional ratio. Moreover, the amplification factor was proportional to the cross-sectional ratio provided the amplification factor did not exceed 4.6. Also, the longitudinal vibration when a static pressing force  $F$  was applied had a resonance frequency corresponding to half of the wavelength of this hollow-type stepped horn length in all cases. The longitudinal vibration distribution and node position were hardly affected by the magnitude of  $F$ . However, impedance increased with  $F$  for all values of the cross-sectional ratio. Also, impedance increased with cross-sectional ratio.

Second, in the case of a horn with diagonal slits, we found that the torsional vibration has a resonance frequency corresponding to three-quarter of the wavelength for this length of hollow-type stepped horn when various conditions. The longitudinal vibration distribution was hardly affected by diagonal slits when the solid part contains diagonal slits. The larger the number of slits, the larger the torsional vibration amplitude at the tip becomes. The torsional vibration amplitude of the tip side increased when the slit part contained the hollow part, the slits bore the hollow part and the slit part was near the node position of longitudinal vibration. The torsional vibration distribution in the range of 0-50 mm attenuated when cross-sectional ratio was large and center position  $x$  of slit part was equal to 50 mm. The torsional vibration amplitude of the tip side was hardly affected by cross-sectional ratio.

## REFERENCES

- 1 H. Miura: "Eggshell Cutter Using Ultrasonic Vibration" *Japanese Journal of Applied Physics* **42**, 2996-2999 (2003)
- 2 H. Miura: "Vibration Characteristics of Stepped Horn Joined Cutting Tip Employed in Circular Cutting Using Ultrasonic Vibration" *Journal of Applied Physics* **47**, 4282-4286 (2008)
- 3 J. Tsujino: "Studies on the Ring Type Magnetic Ultrasonic Vibration Detector" *Journal of Applied Physics Supplement* **23**, pp. 212-214 (1984)
- 4 T. Asami, H. Miura: "Characteristics of longitudinal vibration to cut a circle shape by ultrasonic vibration" *Proceedings of Symposium on Ultrasonic Electronics* **30**, pp. 291 -292 (2009)